


Torsional Vibration Reduction of a Rotor by Using Nonlinear Dual Dynamic Vibration Absorber

Sepehr Goodarzi, Abbas Rahi* 

Faculty of Mechanical and Energy Engineering, Shahid Beheshti University, Tehran, Iran.

ABSTRACT: Torsional vibrations in rotors can lead to fatigue failure and system instability, making effective vibration control critical for industrial applications. This study proposes a nonlinear dual dynamic vibration absorber to mitigate torsional vibrations in a rotor. The absorber consists of two symmetric sets, each comprising a mass, spring, and damper, seamlessly integrated onto the rotor disc for practical implementation. The key equations describing the system's behavior are derived using the Lagrangian method and, due to their nonlinearity, solved using the method of multiple scales. The influence of the absorbers' mass and distance ratios on the torsional vibration amplitude at resonance is investigated, revealing that equal mass and distance ratios optimize performance. Specifically, the absorber reduces the vibration amplitude at resonance from 0.03 radians to 0.5 milliradians. The effect of damping on vibration suppression is also analyzed, and a comparison between linear and nonlinear states demonstrates the superior efficacy of the nonlinear approach. Unlike conventional single or linear absorbers, this dual nonlinear design significantly enhances vibration reduction at resonance, offering improved rotor stability and durability for industrial systems.

Review History:

Received: Mar. 14, 2025

Revised: Jul. 01, 2025

Accepted: Sep. 14, 2025

Available Online: Sep. 20, 2025

Keywords:

Nonlinear Dynamic Vibration Absorber

Rotor

Torsional Vibrations

Method of Multiple Scales

1- Introduction

Torsional vibration systems are prevalent in industrial applications. Due to low damping at resonance frequencies, these systems can experience significant oscillation amplitudes, potentially causing fatigue failure and damage to machine connections. Thus, reducing torsional vibrations is essential for system stability and minimizing equipment damage. One effective method for controlling vibrations, including torsional vibrations, is the use of dynamic vibration absorbers. Frahm [1] introduced the concept of the dynamic vibration absorber, designing a fluid tank to prevent ships' rolling motion. The advantages of Frahm's absorber include ease of installation and simple design. An undamped dynamic vibration absorber provides optimal neutralization at a specific design frequency, making it highly effective when the excitation frequency is constant. However, its effective range is limited, and if the excitation frequency shifts, the system's vibration amplitude may exceed that without the absorber. To address this, Den Hartog and Ormondroyd [2] incorporated damping into the absorber. Iwanami and Seto [3] proposed a dual vibration absorber, demonstrating that it reduces vibration amplitude at resonance more effectively than a conventional absorber. Asami [4] analyzed the dual vibration absorber in series and parallel configurations, optimizing its parameters using various methods. The series

configuration outperformed the parallel configuration, which, in turn, surpassed the conventional absorber in reducing vibration amplitude. Shen et al. [5] developed a dynamic vibration absorber with negative stiffness, where deformation opposes the applied external force, unlike positive stiffness, where deformation aligns with the force. Their absorber, optimized for frequency and damping ratios, significantly reduced vibration amplitude compared to conventional absorbers across various mass ratios. Nazari and Rahi [6] explored the use of a cantilever beam-based nonlinear dynamic absorber with a tip mass to suppress vibrations in a nonlinear system. Shangguan and Pan [7] designed a multi-mass absorber to reduce crankshaft torsional vibrations, modeling the crankshaft as a 15-degree-of-freedom system. Vu et al. [8] optimized a dynamic vibration absorber for torsional vibration reduction, modeling a shaft as single- and multi-degree-of-freedom systems. Their results showed that the absorber reduced vibration amplitude to near zero rapidly. Manchi and Sujatha [9] employed a centrifugal pendulum absorber, attached around a disc in a vehicle's power transmission system, to reduce torsional vibrations. Cao et al. [10] used a nonlinear energy sink to mitigate rotor torsional vibrations, validating results experimentally. Xiang and Wong [11] developed a controllable electromagnetic dynamic absorber for high-speed rotating machinery, allowing adjustable stiffness and damping without structural changes. Nguyen [12] optimized a tuned mass damper for

*Corresponding author's email: a_rahi@sbu.ac.ir

shaft torsional vibrations using the minimum kinetic energy method, validating results numerically. Shen et al. [13] introduced an innovative absorber with grounded stiffness and an amplification mechanism, finding that positive stiffness yielded the best vibration reduction. Wang et al. [14] proposed a multiple absorber for systems under multiple excitations, validated experimentally with a magnetic damper. Chang et al. [15] developed a quasi-zero stiffness absorber for low-frequency vibrations, outperforming conventional absorbers under random and impact excitations. Chung and Wang [16] studied an unconventional absorber with a damper connected to the ground, optimized using the fixed-point method, which outperformed conventional absorbers. Tchokogoué et al. [17] analyzed a centrifugal dynamic absorber, considering gravity effects significant at low rotational speeds. Rao and Sujatha [18] designed a centrifugal pendulum absorber to reduce both axial and torsional vibrations of a rotating shaft. Kecik [19] proposed a system combining vibration reduction and energy harvesting, integrating an energy harvesting device within a pendulum absorber without compromising performance. El-Sayed and Baoumy [20] mitigated nonlinear system vibrations under multifrequency excitation, identifying critical conditions when internal and subharmonic resonances occur simultaneously. Shaw and Bahadori [21] investigated a pendulum absorber in fluid, analyzing fluid pressure effects on performance. Abu Seer et al. [22] introduced an adaptive absorber for torsional vibrations in rotating equipment, effective across varying frequencies and compatible with multi-degree-of-freedom systems. Faal et al. [23] proposed a simple, undamped absorber for shaft torsional vibrations, mounted with fixed supports to maintain balance. Goodarzi and Rahi [24] optimized a dual dynamic vibration absorber using the Lagrangian method and genetic algorithm to reduce torsional vibrations. Taghipour et al. [25] investigated the vibration mitigation of a nonlinear Jeffcott rotor system using linear (TMD), nonlinear (NES), and combined (TMD-NES) vibration absorbers. The authors employ semi-analytical and numerical methods to analyze the system's dynamics, demonstrating that all three absorbers effectively reduce vibrations, with TMD-NES offering the best performance and stability. The research highlights the importance of optimizing absorber parameters to enhance robustness against variations in system conditions. Cao et al. [26] introduced an inerter-enhanced nonlinear energy sink (INES) to suppress torsional vibrations in rotor systems. By combining a nonlinear energy sink (NES) with an inerter, the system reduces the reliance on heavy inertial mass compared to conventional designs. Al-Bedoor et al. [27] propose a dynamic absorber to reduce torsional vibrations in synchronous motor-driven systems, consisting of two inertia rings connected by spring-like elements, which significantly reduces vibration amplitude and duration through optimal tuning. Their results demonstrate the absorber's effectiveness in mitigating torsional vibrations during motor startup.

This study employs absorbers to mitigate rotor torsional vibrations, positioned symmetrically at a defined distance on the rotor disk. A key innovation is the nonlinear and dual

characteristics of the dynamic vibration absorber, designed to effectively reduce torsional vibrations through dual linear oscillatory motion.

2- Modeling and derivation of equations

The primary vibration system consists of a rotor that is rotating at a constant angular velocity Ω and subjected to an oscillating external torque $\tilde{A}(t) = \tilde{A}_0 e^{i\omega t}$. The radius and mass of the disk are R and M , respectively, with the moment of inertia J and the torsional stiffness of the shaft k_t . B_1 and B_2 are bearings. To prevent imbalance, a dynamic vibration absorber is implemented as two symmetric sets of mass, spring, and damper with similar performance. These absorbers have masses m_1 and m_2 , spring stiffnesses k_1 and k_2 , and dampers with damping coefficients c_1 and c_2 , embedded in the disk. The distances of the absorbers from the center of the disk are d_1 and d_2 , and their displacements are u and v . The dynamic vibration absorber is designed to reduce the torsional vibrations of the rotor through its linear oscillatory motion. The degrees of freedom of the system are θ , u and v . Figs. 1 and 2 show the side view and front view of the system, respectively.

The kinetic energy of the system, described in Eq. (1), includes the kinetic energy of both the disk and the absorbers:

$$KE = \frac{1}{2}(J)\dot{\theta}^2 + \frac{1}{2}(2m_1)v_{m1}^2 + \frac{1}{2}(2m_2)v_{m2}^2 \quad (1)$$

The velocities \vec{v}_{m1} and \vec{v}_{m2} will be as follows:

$$\begin{aligned} \vec{v}_{m1} &= -\dot{u}\hat{i} + \dot{\theta}\hat{k}(d_1\hat{j} - u\hat{i}) \\ \vec{v}_{m2} &= \dot{v}\hat{j} + \dot{\theta}\hat{k}(d_2\hat{i} + v\hat{j}) \end{aligned} \quad (2)$$

After substituting \vec{v}_{m1} and \vec{v}_{m2} into Eq. (1):

$$KE = \frac{1}{2}J\dot{\theta}^2 + (m_1)[(-u\dot{\theta})^2 + (-\dot{u} - d_1\dot{\theta})^2] + (m_2)[(-v\dot{\theta})^2 + (\dot{v} + d_2\dot{\theta})^2] \quad (3)$$

The system's potential energy comprises the combined potential energy of the absorber springs and the torsional stiffness of the shaft.

$$PE = 4\left(\frac{1}{2}k_1u^2\right) + 4\left(\frac{1}{2}k_2v^2\right) + \frac{1}{2}k_t\theta^2 \quad (4)$$

Using the system's kinetic energy and potential energy, the Lagrangian is expressed as:

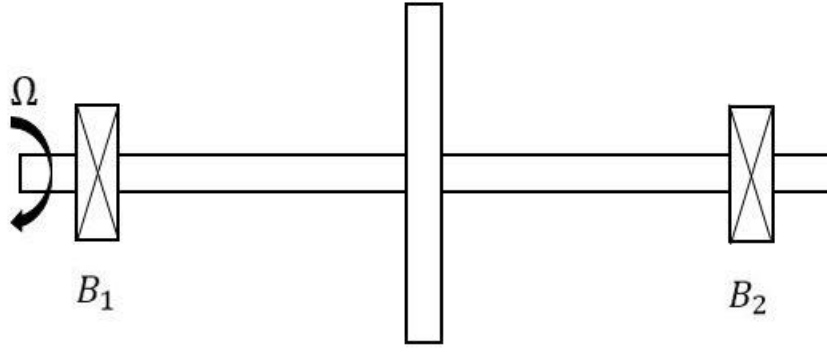


Fig. 1. The side view of the rotor

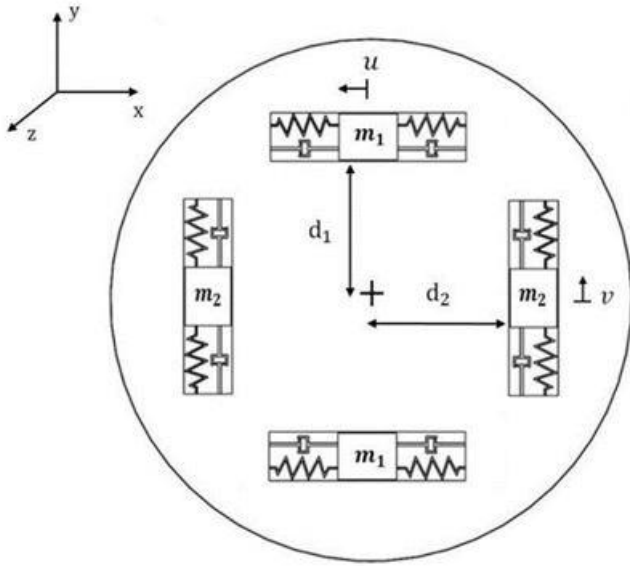


Fig. 2. The front view of the disk

$$\begin{aligned}
 L = KE - PE = & \frac{1}{2} J \dot{\theta}^2 \\
 & + (m_1) [(-u\dot{\theta})^2 + (-\dot{u} - d_1\dot{\theta})^2] \\
 & + (m_2) [(-v\dot{\theta})^2 + (\dot{v} + d_2\dot{\theta})^2] \\
 & - 2k_1 u^2 - 2k_2 v^2 - \frac{1}{2} k_t \theta^2
 \end{aligned} \quad (5)$$

The Lagrange equation is given by [28]:

$$\frac{d}{dt} \left(\frac{\partial L}{\partial \dot{q}_i} \right) - \frac{\partial L}{\partial q_i} = Q_i, \quad (i = 1, 2), \quad \begin{cases} q_1 = \theta \\ q_2 = u \\ q_3 = v \end{cases} \quad (6)$$

Non-conservative forces Q_1 , Q_2 and Q_3 are equal to:

$$\begin{cases} Q_1 = \Gamma(t) \\ Q_2 = -4c_1 \dot{u} \\ Q_3 = -4c_2 \dot{v} \end{cases} \quad (7)$$

By applying Lagrange's equation, incorporating the system's kinetic energy, potential energy, and non-conservative forces, the equations of motion are derived as follows:

$$\begin{aligned}
 & (J + 2m_1 u^2 + 2m_1 d_1^2 + 2m_2 v^2 + 2m_2 d_2^2) \ddot{\theta} \\
 & + 2m_1 d_1 \ddot{u} + 4m_1 u \dot{u} \dot{\theta} + 2m_2 d_2 \ddot{v} \\
 & + 4m_2 v \dot{v} \dot{\theta} + k_t \theta = \Gamma(t)
 \end{aligned} \quad (8)$$

$$m_1 \ddot{u} + m_1 d_1 \ddot{\theta} - m_1 u \dot{\theta}^2 + 2c_1 \dot{u} + 2k_1 u = 0$$

$$m_2 \ddot{v} + m_2 d_2 \ddot{\theta} - m_2 v \dot{\theta}^2 + 2c_2 \dot{v} + 2k_2 v = 0$$

3-Solving nonlinear equations using the method of multiple scales

Due to the nonlinearity of the equations of motion, an analytical solution is sought using the method of multiple scales [29, 30]. This method is well-suited for systems exhibiting small amplitudes of vibration. The nonlinear governing equations are:

$$\begin{aligned}
 & \ddot{\theta} + \varepsilon \alpha_1 u \dot{\theta} + \varepsilon \alpha_2 v \dot{\theta} + \varepsilon \beta_1 \ddot{u} \\
 & + \varepsilon \beta_2 \ddot{v} + \omega_1^2 \theta = \varepsilon f e^{i\Omega T_0} \\
 & \ddot{u} + \varepsilon d_1 \ddot{\theta} - u \dot{\theta}^2 + 2\varepsilon \zeta_1 \omega_2 \dot{u} + \omega_2^2 u = 0 \\
 & \ddot{v} + \varepsilon d_2 \ddot{\theta} - v \dot{\theta}^2 + 2\varepsilon \zeta_2 \omega_3 \dot{v} + \omega_3^2 v = 0
 \end{aligned} \quad (9)$$

Because the governing equations are nonlinear, the normalized system parameters are:

$$\begin{aligned}\alpha_1 &= \frac{4m_1}{J + 2m_1d_1^2 + 2m_2d_2^2}, \\ \varepsilon\alpha_2 &= \frac{4m_2}{J + 2m_1d_1^2 + 2m_2d_2^2}, \\ \omega_1^2 &= \frac{k_1}{J + 2m_1d_1^2 + 2m_2d_2^2}, \\ \omega_2^2 &= \frac{2k_1}{m_1}, \omega_3^2 = \frac{2k_2}{m_2}, \\ \varepsilon\zeta_1 &= \frac{c_1}{\sqrt{2k_1m_1}}, \varepsilon\zeta_2 = \frac{c_2}{\sqrt{2k_2m_2}}, \\ \varepsilon\beta_1 &= \frac{2m_1d_1}{J + 2m_1d_1^2 + 2m_2d_2^2}, \\ \varepsilon\beta_2 &= \frac{2m_2d_2}{J + 2m_1d_1^2 + 2m_2d_2^2}\end{aligned}$$

In Eq. (9), A small bookkeeping parameter ε is used, indicative of a small vibration amplitude. By definition, $T_n = \varepsilon^n t$, $T_0 = t$ and $T_1 = \varepsilon t$ that are fast and slow time scales, respectively. Also θ_0 , u_0 and v_0 are displacement functions in order ε^0 and θ_1 , u_1 and v_1 displacement functions in order ε^1 .

$$\theta = \theta_0(T_0, T_1) + \varepsilon\theta_1(T_0, T_1) + \dots$$

$$u = u_0(T_0, T_1) + \varepsilon u_1(T_0, T_1) + \dots \quad (10)$$

$$v = v_0(T_0, T_1) + \varepsilon v_1(T_0, T_1) + \dots$$

Using the definition $D_n = \frac{\partial}{\partial T_n}$, for the slow time scales, the total time derivative operator is given by the following expansion:

$$\frac{d}{dt} = D_0 + \varepsilon D_1, \frac{d^2}{dt^2} = D_0^2 + 2\varepsilon D_0 D_1 \quad (11)$$

In the perturbation analysis, the relationship between the primary system's excitation frequency, the natural frequencies of the system, and the parameters of the nonlinear dynamic absorber is defined in terms of specific internal and external parameters. $\dot{U} = \omega_1 + \varepsilon\sigma_1$, $\omega_1 = \omega_2 + \varepsilon\sigma_2$, $\omega_1 = \omega_3 + \varepsilon\sigma_3$ [31].

By replacing $\theta(T_0, T_1)$, $u(T_0, T_1)$ and $v(T_0, T_1)$ in the equations of nonlinear motion of the system, and by separating

the system of equations based on the powers of zero and one ε , the system of equations is obtained:

$$\varepsilon^0 : D_0^2 \theta_0 + \omega_1^2 \theta_0 = 0 \quad (12)$$

$$\varepsilon^0 : D_0^2 u_0 + \omega_2^2 u_0 = 0 \quad (13)$$

$$\varepsilon^0 : D_0^2 v_0 + \omega_3^2 v_0 = 0 \quad (14)$$

$$\begin{aligned}\varepsilon^1 : D_0^2 \theta_1 + \omega_1^2 \theta_1 + 2D_0 D_1 \theta_0 \\ + \alpha_1 u_0 (D_0 u_0) (D_0 \theta_0) + \alpha_2 v_0 (D_0 v_0) (D_0 \theta_0) \\ + \beta_1 D_0^2 u_0 + \beta_2 D_0^2 v_0 = f e^{i\Omega T_0}\end{aligned} \quad (15)$$

$$\begin{aligned}\varepsilon^1 : D_0^2 u_1 + \omega_2^2 u_1 + 2D_0 D_1 u_0 + d_1 D_0^2 \theta_0 \\ - u_0 (D_0 \theta_0)^2 + 2\zeta_1 \omega_2 D_0 u_0 = 0\end{aligned} \quad (16)$$

$$\begin{aligned}\varepsilon^1 : D_0^2 v_1 + \omega_3^2 v_1 + 2D_0 D_1 v_0 + d_1 D_0^2 \theta_0 \\ - v_0 (D_0 \theta_0)^2 + 2\zeta_2 \omega_3 D_0 v_0 = 0\end{aligned} \quad (17)$$

The harmonic response of equations (12) and (14) in polar form is:

$$\theta_0 = A(T_1) e^{i\omega_1 T_0} + \bar{A}(T_1) e^{-i\omega_1 T_0} \quad (18)$$

$$u_0 = B(T_1) e^{i\omega_2 T_0} + \bar{B}(T_1) e^{-i\omega_2 T_0} \quad (19)$$

$$v_0 = C(T_1) e^{i\omega_3 T_0} + \bar{C}(T_1) e^{-i\omega_3 T_0} \quad (20)$$

The above relation $\bar{A}(T_1)$, $\bar{B}(T_1)$ and $\bar{C}(T_1)$ are the complex conjugates of the amplitude $A(T_1)$, $B(T_1)$ and $C(T_1)$ respectively. By replacing the polar responses in Eqs. (15) and (17) have:

$$\begin{aligned}D_0^2 \theta_1 + \omega_1^2 \theta_1 = -2i \omega_1 A'(T_1) e^{i\omega_1 T_0} \\ - \alpha_1 (-\omega_1 \omega_2 A B^2 e^{i(\omega_1 + 2\omega_2) T_0} + \omega_1 \omega_2 \bar{A} \bar{B}^2 e^{i(2\omega_2 - \omega_1) T_0}) \\ - \alpha_2 (-\omega_1 \omega_3 A C^2 e^{i(\omega_1 + 2\omega_3) T_0} + \omega_1 \omega_3 \bar{A} \bar{C}^2 e^{i(2\omega_3 - \omega_1) T_0}) \\ + \beta_1 \omega_2^2 B e^{i\omega_2 T_0} + \beta_2 \omega_3^2 C e^{i\omega_3 T_0} \\ + f e^{i\Omega T_0} + CC\end{aligned} \quad (21)$$

$$\begin{aligned}
D_0^2 u_1 + \omega_2^2 u_1 &= -2i \omega_2 B'(T_1) e^{i \omega_2 T_0} \\
&+ d_1 \omega_1^2 A e^{i \omega_1 T_0} + \omega_1^2 A^2 \bar{B} e^{i(2\omega_1 - \omega_2)T_0} \\
&+ \omega_1^2 A \bar{A} B e^{i \omega_2 T_0} - 2i \zeta_1 \omega_2^2 B e^{i \omega_2 T_0} + CC
\end{aligned} \quad (22)$$

$$\begin{aligned}
D_0^2 v_1 + \omega_3^2 v_1 &= -2i \omega_3 C'(T_1) e^{i \omega_3 T_0} \\
&+ d_2 \omega_1^2 A e^{i \omega_1 T_0} + \omega_1^2 A^2 \bar{C} e^{i(2\omega_1 - \omega_3)T_0} \\
&+ \omega_1^2 A \bar{A} C e^{i \omega_3 T_0} - 2i \zeta_2 \omega_3^2 C e^{i \omega_3 T_0} + CC
\end{aligned} \quad (23)$$

The term CC in the preceding equations represents the complex conjugate. The amplitudes of $A(T_1)$, $B(T_1)$ and $C(T_1)$ are expressed in polar coordinates by relations:

$$A(T_1) = \frac{1}{2} a(T_1) e^{i \delta(T_1)} \quad (24)$$

$$B(T_1) = \frac{1}{2} b(T_1) e^{i \gamma(T_1)} \quad (25)$$

$$C(T_1) = \frac{1}{2} c(T_1) e^{i \psi(T_1)} \quad (26)$$

Substituting this relation into Equations (21) and (22) and eliminating the secular terms results in:

$$\begin{aligned}
&-i \omega_1 a' + \omega_1 a \delta' - \frac{1}{8} \alpha_1 \omega_1 \omega_2 a b^2 e^{2i \phi_2} \\
&- \frac{1}{8} \alpha_2 \omega_1 \omega_3 a c^2 e^{2i \phi_3} + \beta_1 \omega_2^2 b e^{i \phi_2} \\
&+ \beta_2 \omega_3^2 c e^{i \phi_3} + f e^{i \phi_1} = 0
\end{aligned} \quad (27)$$

$$\begin{aligned}
&-i \omega_2 b' + \omega_2 b \gamma' - 2i \zeta_1 \omega_2^2 b \\
&+ d_1 \omega_1^2 a e^{-i \phi_2} - \omega_1^2 a b^2 e^{-2i \phi_2} = 0
\end{aligned} \quad (28)$$

$$\begin{aligned}
&-i \omega_3 c' + \omega_3 c \psi' - 2i \zeta_2 \omega_3^2 c \\
&+ d_2 \omega_1^2 a e^{-i \phi_3} - \omega_1^2 a c^2 e^{-2i \phi_3} = 0
\end{aligned} \quad (29)$$

In relations (27) to (29), it is, $\phi_1 = \sigma_1 T_1 - \delta$, $\phi_2 = \gamma - \delta - \sigma_2 T_1$ and $\phi_3 = \psi - \delta - \sigma_3 T_1$. To obtain the steady-state response, the derivatives with respect to T_1 , namely $a', b', c', \delta', \gamma'$ and ψ' are set to zero in Equations (27) and (29). The system's stability is then determined by solving the equations resulting from setting both the real and

imaginary parts of this modified system to zero.

By equating the real and imaginary parts of the equations to zero, we will have a stable response:

$$\begin{aligned}
&\omega_1 a \delta' - \frac{1}{8} \alpha_1 \omega_1 \omega_2 a b^2 \cos 2\phi_2 \\
&- \frac{1}{8} \alpha_2 \omega_1 \omega_3 a c^2 \cos 2\phi_3 + f \cos \phi_1 \\
&+ \beta_1 \omega_2^2 b \cos \phi_2 + \beta_2 \omega_3^2 c \cos \phi_3 = 0
\end{aligned} \quad (30)$$

$$\begin{aligned}
&- \frac{1}{8} \alpha_1 \omega_1 \omega_2 a b^2 \sin 2\phi_2 - \frac{1}{8} \alpha_2 \omega_1 \omega_3 a c^2 \sin 2\phi_3 \\
&+ f \sin \phi_1 + \beta_1 \omega_2^2 b \sin \phi_2 + \beta_2 \omega_3^2 c \sin \phi_3 = 0
\end{aligned} \quad (31)$$

$$\omega_2 b \gamma' + d_1 \omega_1^2 a \cos \phi_2 - \omega_1^2 a b^2 \cos 2\phi_2 = 0 \quad (32)$$

$$-2\zeta_1 \omega_2^2 b - d_1 \omega_1^2 a \sin \phi_2 + \omega_1^2 a b^2 \sin 2\phi_2 = 0 \quad (33)$$

$$\omega_3 c \psi' + d_2 \omega_1^2 a \cos \phi_3 - \omega_1^2 a c^2 \cos 2\phi_3 = 0 \quad (34)$$

$$-2\zeta_2 \omega_3^2 c - d_2 \omega_1^2 a \sin \phi_3 + \omega_1^2 a c^2 \sin 2\phi_3 = 0 \quad (35)$$

To solve the nonlinear Eqs. (30–35) Derived from the multiple scales method, the Newton-Raphson method [32, 33] was employed due to its high convergence rate for nonlinear systems with a limited number of variables. These equations, representing the steady-state response of the system, were reformulated as a system of nonlinear equations $F(x) = 0$, where x is the vector of unknown variables. The Newton-Raphson method was initiated with carefully selected initial guesses for x , informed by preliminary linear analysis Eqs. (18–20). The Jacobian matrix (J), comprising partial derivatives of F with respect to x , was computed to update the solution iteratively via $X_{n+1} = X_n - J^{-1}(X_n) \cdot F(X_n)$. This process was implemented in MATLAB using the standard function `fsolve`, with a convergence criterion of 10^{-6} , ensuring high-precision steady-state solutions [29, 30]. It was assumed that the initial guesses were sufficiently close to the true solutions to guarantee rapid convergence. This approach enabled accurate computation of the system's response, facilitating the generation of results presented in Figs. 4–8.

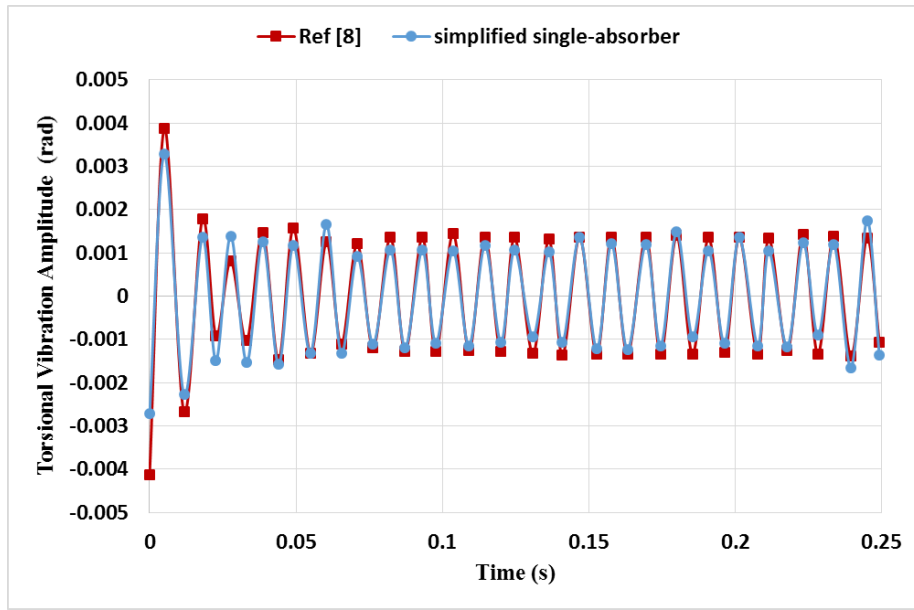
4- Numerical results and validation

For the numerical analysis of the system's performance and validation, the rotor specifications are considered in accordance with the study by Vu et al. [8].

To validate the results of the proposed nonlinear dual dynamic vibration absorber, a validation study was

Table 1. Rotor specifications [8]

Parameters	Value	Unit
R	14	cm
M	5	kg
k_t	10000	Nm/rad
Γ_0	5	N.m

**Fig. 3. Comparison of torsional vibration amplitude versus time for the simplified single-absorber system and Vu et al. [8]**

conducted by simplifying the system to align with the linear single-degree-of-freedom model in Vu et al. [8]. The second absorber was removed, resulting in a system with a single absorber, as in [8]. The governing nonlinear equations were linearized around the equilibrium position by neglecting higher-order nonlinear terms and assuming harmonic oscillatory motion of the single absorber, consistent with [8]. All system parameters were adopted directly from [8] to ensure an accurate comparison. The linearized equations were solved numerically using the Newton-Raphson method, ensuring high numerical precision.

The torsional vibration amplitude of the rotor was computed as a function of time under an external excitation torque $\tilde{A}(t) = \tilde{A}_0 e^{i\omega t}$ at the resonance frequency. Fig. 3 presents a time-domain plot comparing theta for the simplified system with the results reported in [8]. Both systems exhibit an initial transient response with a peak amplitude of approximately 0.004 radians, followed by a rapid stabilization to a steady-

state amplitude of about 0.001 radians within 0.05 seconds. The steady-state amplitude of the simplified system closely matches that of [8], with a maximum deviation of less than 7% (approximately 0.0001–0.0002 radians), confirming the accuracy of the dynamic modeling and numerical approach used in this study. This validation study establishes a robust baseline by replicating the results of [8] with the simplified system, confirming the correctness of the proposed modeling and numerical methods.

The nonlinear dynamic vibration absorber examined in this study is modeled as multiple units, as shown in Figs. 1 and 2, consisting of four sets of mass, spring, and damper. To maintain symmetry and balance of the rotor, the absorbers are paired with identical performance. That is, the absorbers in front of each other have similar characteristics and are equidistant from the rotor's center. Based on the system specifications in Table 1, the absorber's performance is evaluated at the resonance frequency to achieve optimal

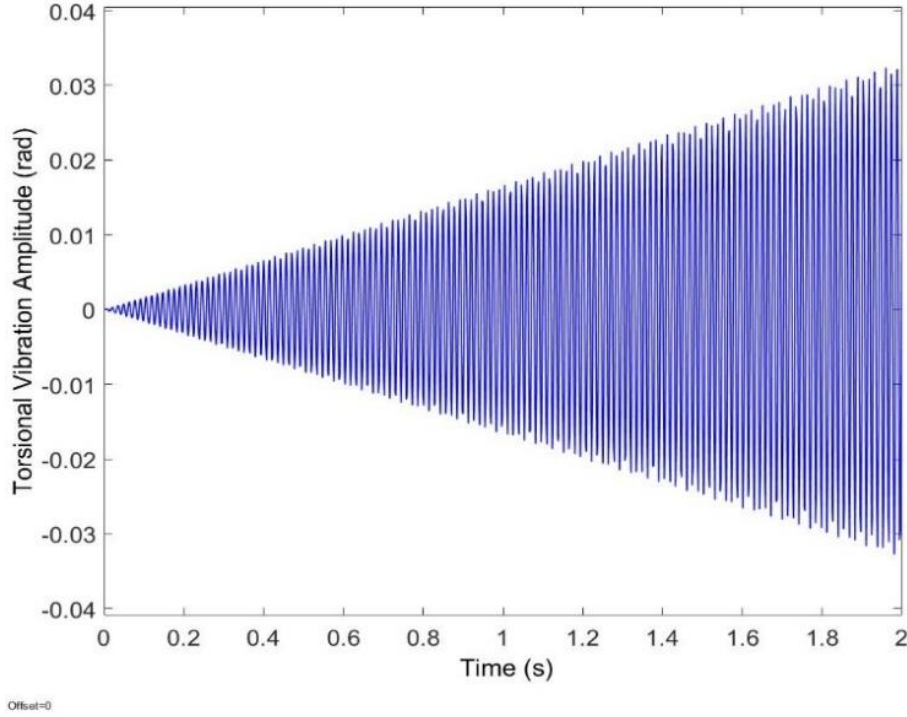


Fig. 4. The amplitude of the rotor's torsional vibrations without the absorber at resonance

performance under critical conditions. The system's natural frequency without the dynamic vibration absorber is $\omega_n = 447.21 \text{ rad/s}$. Fig. 4 shows the amplitude of the rotor's torsional vibrations without the absorber at resonance over the time interval from 0 to 2 seconds.

After adding the absorbers to the rotor, it is essential to determine how the masses of the absorbers relate to each other due to their dual nature. The impact of having equal or unequal absorber masses on their performance and the reduction of torsional vibrations must be assessed. It is noteworthy that for optimal absorber performance, their design should ensure that their natural frequency matches the resonance frequency. According to the equations, the natural frequency of each absorber will be as follows:

$$\omega_2^2 = \frac{2k_1}{m_1}, \omega_3^2 = \frac{2k_2}{m_2}$$

It is worth mentioning that the natural frequency of the main system after the addition of the absorbers is as follows:

$$\omega_1^2 = \frac{k_t}{J + 2m_1d_1^2 + 2m_2d_2^2}$$

The mass ratio of the first absorber with mass m_1 to the second absorber with mass m_2 is given by:

$$\mu = \frac{m_1}{m_2}$$

To examine the effect of changes in μ on the reduction of the rotor's torsional vibration amplitude, other components remain constant, and the absorbers are positioned 10 cm from the center of the rotor. By varying the mass ratio of the absorbers to maintain the natural frequency of each absorber and preserve its performance at resonance, the stiffness of the absorbers will also change accordingly. The reduction in the rotor's torsional vibration amplitude with increasing mass ratio (μ), as shown in Figure 5, is attributed to the enhanced energy transfer from the rotor to the absorbers. When the mass ratio approaches unity ($\mu = 1$) the absorbers' masses are equal, optimizing the system's moment of inertia and allowing both absorbers to oscillate in phase with the rotor's resonance frequency. This synchronization maximizes the absorption of vibrational energy, reducing the rotor's amplitude from 0.03 radians to 0.5 milliradians. Physically, equal masses ensure balanced dynamic forces, minimizing residual vibrations and stabilizing the system at resonance.

Figure 6 illustrates that the vibration amplitude of the absorbers varies with the mass ratio (μ). When $\mu = 1$, both absorbers exhibit identical amplitudes due to their equal masses, which promotes symmetric energy distribution.

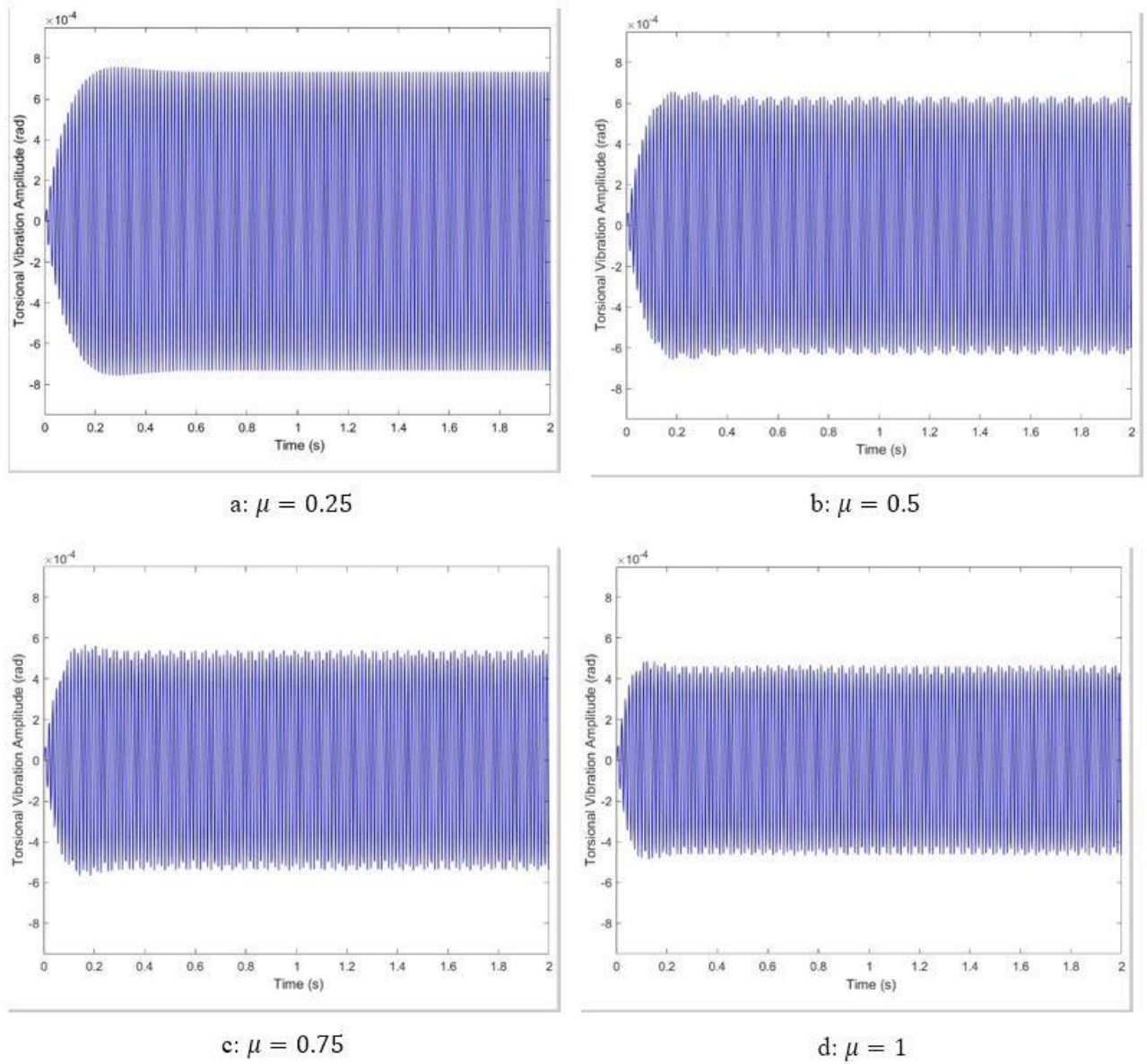


Fig. 5. The amplitude of the rotor's torsional vibrations at different mass ratios of absorbers

Physically, this symmetry ensures that each absorber equally shares the vibrational energy transferred from the rotor, reducing the risk of localized stress. For unequal mass ratios (e.g., $\mu = 0.25$), the lighter absorber oscillates with a higher amplitude to compensate for its lower inertia, while the heavier absorber absorbs more energy, highlighting the dynamic interplay between mass and energy dissipation.

Another factor that affects the torsional vibration amplitude of the rotor is the ratio of the distances between the absorbers. The distance of the first absorber from the rotor center is d_1 and the distance of the second absorber is d_2 . It needs to be determined how the ratio of these distances should be to achieve the best performance. For this purpose, the following parameter is considered as the ratio of the

distances of the absorbers.

$$\eta = \frac{d_1}{d_2}$$

As shown in Fig. 7, the torsional vibration amplitude decreases as the distance ratio (η) approaches unity. This behavior is due to the symmetric placement of absorbers ($\eta = 1$), which maintains dynamic balance by ensuring equal moment arms relative to the rotor's center. Physically, equal distances optimize the torque cancellation, as the absorbers' oscillatory forces counteract the rotor's vibrations uniformly. This configuration minimizes additional stresses on the shaft, reducing the amplitude from 0.6 milliradians to 0.4 milliradians, enhancing system stability at resonance.

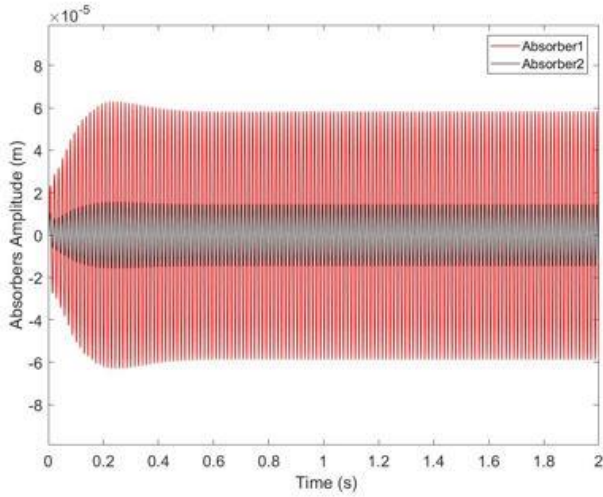
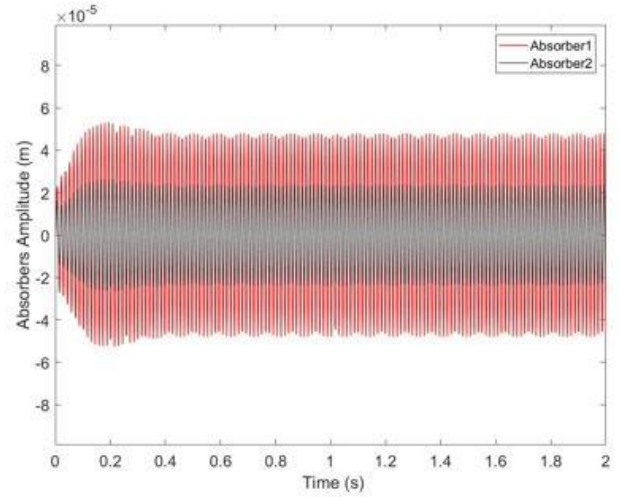
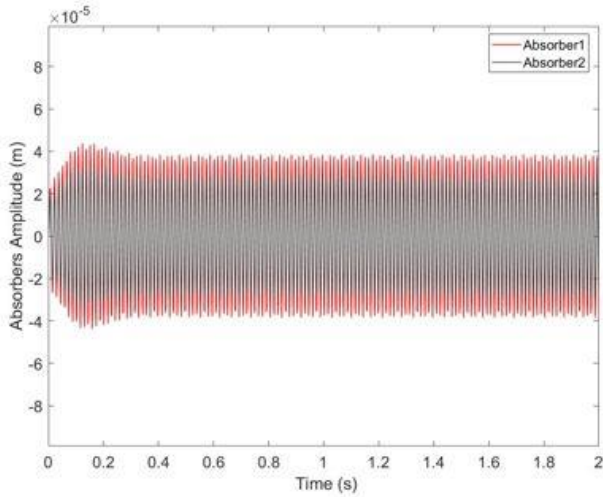
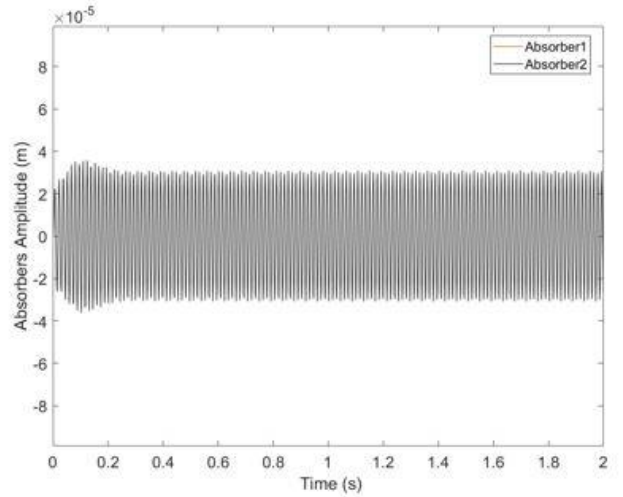
a : $\mu = 0.25$ b : $\mu = 0.5$ c : $\mu = 0.75$ d : $\mu = 1$ **Fig. 6. Vibration amplitude of absorbers with different mass ratios**

Figure 8 shows that the absorbers' vibration amplitudes depend on their distance ratio (η). When $\eta = 1$, both absorbers oscillate with equal amplitudes due to their symmetric positioning, which balances the dynamic forces acting on the rotor disc. Physically, an absorber closer to the rotor's center (e.g., $\eta = 0.25$) experiences a smaller moment arm, resulting in lower amplitude, while a farther absorber has a larger amplitude due to increased leverage. This variation reflects the absorbers' role in redistributing vibrational energy, with equal distances optimizing energy absorption and system equilibrium.

After separately examining the effects of distance ratio and mass ratio on the torsional vibration amplitude of the rotor, the simultaneous effect of these two ratios is now

investigated. The non-dimensional torsional vibration amplitude of the rotor is expressed as follows.

$$A = \frac{\theta \times k_t}{\tilde{A}_0}$$

In this context, A represents the non-dimensional torsional vibration amplitude, θ is the torsional vibration amplitude of the rotor in radians, k_t is the torsional stiffness of the shaft, and \tilde{A}_0 is the amplitude of the external excitation torque. Fig. 9 demonstrates that the non-dimensional torsional vibration amplitude is minimized when both mass and distance ratios are unity ($\mu = 1, \eta = 1$). Physically, this optimal condition aligns the absorbers' natural frequencies with the rotor's resonance frequency, maximizing energy transfer.

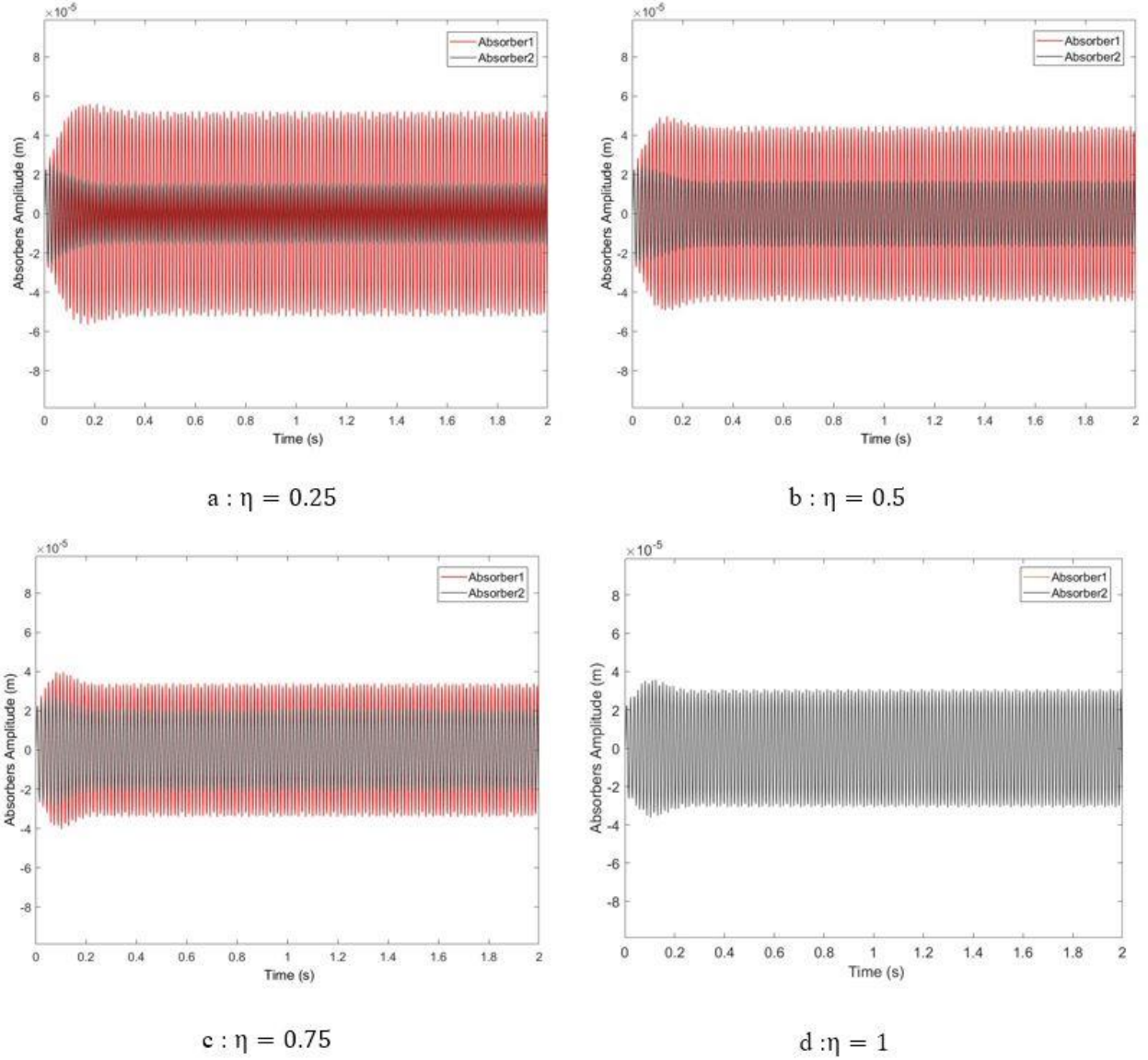


Fig. 8. Vibration amplitude of absorbers with different distance ratios

Equal masses and distances ensure a balanced moment of inertia and symmetric force distribution, reducing dynamic imbalances. This configuration effectively dissipates vibrational energy, preventing amplification of rotor oscillations. The increased amplitude at lower ratios (e.g., $\mu = 0.25$, $\eta = 0.25$) reflects insufficient energy absorption due to suboptimal inertial and geometric properties.

Given that the rotor specifications are selected based on reference [8], the performance of absorbers in the present study under optimal performance is compared with that reference. In this study, a dual absorber is used, and the modeling approach of the absorber is such that it results in the nonlinearity of the governing system equations. The

specifications of absorbers with the appropriate configuration that have the greatest effect in reducing the torsional vibrations of the system are as follows(Table 2):

Fig. 10 highlights the superior performance of the proposed absorber compared to reference [8], reducing torsional vibrations more effectively at resonance. The symmetric arrangement and nonlinear stiffness allow the absorbers to adapt to varying dynamic conditions, absorbing energy that would otherwise amplify rotor vibrations. This results in a significant reduction in amplitude (to 0.5 milliradians), as the nonlinear dynamics counteract the rotor's oscillatory motion more effectively than traditional linear absorbers, ensuring greater system stability.

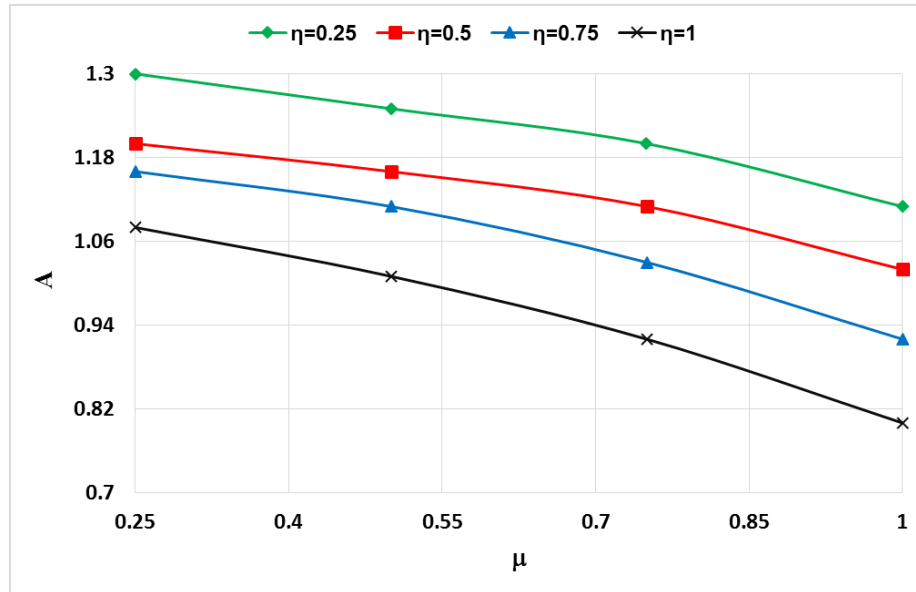


Fig. 9. Simultaneous analysis of the effect of mass ratio and distance ratio of absorbers on non-dimensional torsional vibration amplitude

Table 2. The specifications of absorbers

Parameters	Value	Unit
$m_1 = m_2$	0.1	kg
$d_1 = d_2$	12	cm
$k_1 = k_2$	10000	N/m
$c_1 = c_2$	20	N.s/m

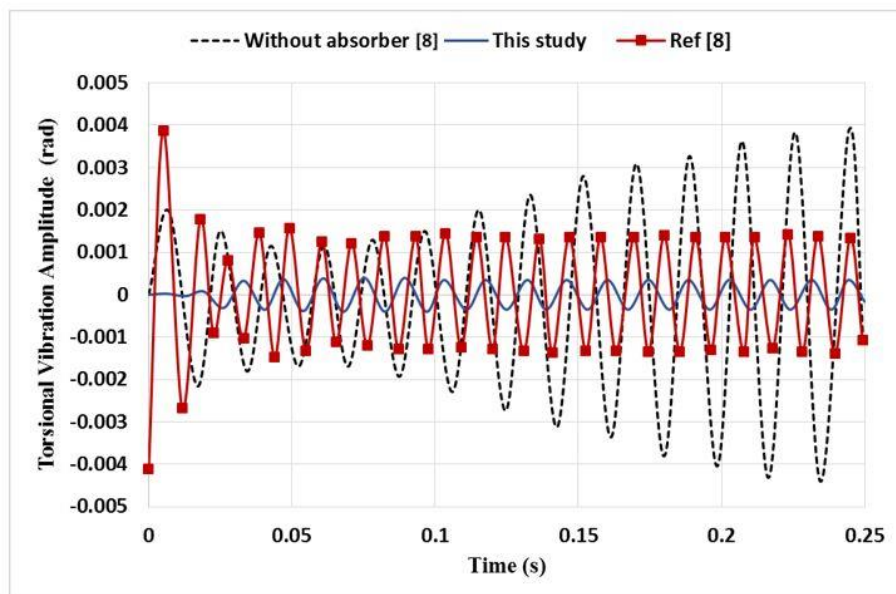


Fig. 10. Performance evaluation of the absorber in the current study

5- Implementation Plan

To realize the proposed nonlinear dynamic vibration absorber in practice, the following phases are considered:

• Initial absorber geometry design

The basic configuration of the absorber (mass, spring, and damper layout) is defined considering symmetry, mass distribution, and spatial constraints on the rotor disk.

• Dynamic modeling

Using the physical properties of the rotor-absorber system, the equations of motion are derived based on Lagrange's formulation, capturing all degrees of freedom and interaction terms.

• Nonlinear analysis

Due to the inherent nonlinear coupling in the system, the equations are solved analytically using the Method of Multiple Scales (MMS), which allows for capturing resonance and amplitude-dependent behavior.

• Parameter adjustment

Key parameters such as damping coefficients, mass ratio, and absorber placement are tuned iteratively to minimize torsional vibration amplitude under resonance conditions.

• Numerical Testing & Comparison

After solving the equations and performing parameter adjustment, numerical analysis is conducted to evaluate the absorber's effectiveness in reducing the rotor's torsional vibrations.

• Fabrication & Experimental Testing

After parameter adjustment, the steady-state equations obtained via the Method of Multiple Scales are solved numerically using the Newton–Raphson method. The torsional response is evaluated for various absorber setups. Results are compared with baseline and literature to confirm effectiveness.

The implementation plan is illustrated as a flowchart in the figure 11.

6- Conclusion

This study introduced a nonlinear dual dynamic vibration absorber to mitigate torsional vibrations in a rotor at resonance frequency. Using the Lagrangian method to derive the governing equations and the method of multiple scales to solve their nonlinear behavior, the effects of the absorbers' mass and distance ratios on torsional vibration amplitude were investigated. The results demonstrated that absorbers with equal mass and distance ratios ($\mu = 1$, $\eta = 1$) achieve optimal performance, reducing the torsional vibration amplitude at resonance from 0.03 radians to 0.5 milliradians. This significant reduction is attributed to the effective transfer of vibrational energy from the rotor to the absorbers, facilitated by tuning the absorbers' natural frequency to match the system's

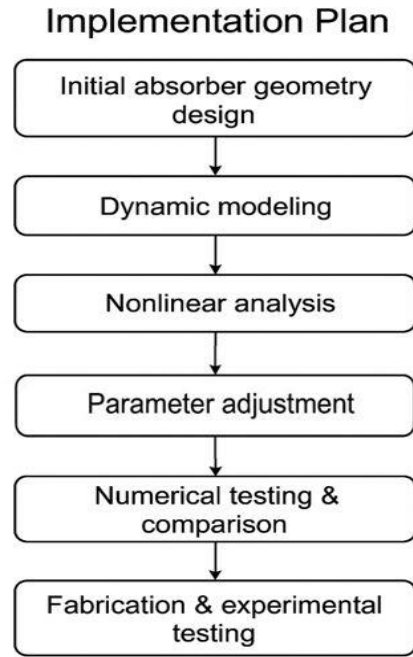


Fig. 11. The implementation plan

resonance frequency. Additionally, the analysis of damping effects revealed that dampers enhance system stability at resonance by dissipating vibrational energy. A comparison between linear and nonlinear states confirmed the superior performance of the nonlinear approach, as it better addresses the complex dynamic behavior of the rotor. These findings have significant implications for industrial applications, as reducing torsional vibrations can extend rotor lifespan and lower maintenance costs. Compared to the reference study [8], the proposed absorber in this work exhibits better performance at resonance, owing to its dual nonlinear design and symmetric placement on the rotor disc. From a physical perspective, employing absorbers with equal mass and distance ratios optimizes the system's moment of inertia and maintains dynamic balance, thereby minimizing stresses on the shaft and connected components. For future research, experimental validation of the absorber's performance under real-world conditions is recommended to assess the impact of factors such as varying rotational speeds or environmental conditions. Extending the model to multi-degree-of-freedom systems or applying it to complex industrial systems, such as turbines or engines, could broaden its applicability. Furthermore, investigating nonlinear damping or variable spring stiffness could enhance the absorber's effectiveness. This study, by introducing a novel dual nonlinear absorber design, represents a significant step toward improving the stability and efficiency of rotating systems.

Nomenclature list

Symbol	Description	Unit
θ	Torsional vibration of the rotor	rad
u, v	displacement of the first and second absorbers	m
m_1, m_2	Mass of the first and second absorbers	kg
k_1, k_2	Spring stiffness of the first and second absorbers	N/m
c_1, c_2	Damping coefficient of the first and second absorbers	N·s/m
μ	Mass ratio of	Dimensionless
η	Distance ratio of absorbers	Dimensionless
$\omega_1, \omega_2, \omega_3$	Natural frequencies of the system and absorbers	rad/s
ε	Small nonlinear parameter	Dimensionless
J	Moment of inertia of the rotor	kg·m ²
k_t	Torsional stiffness of the shaft	N·m/rad
$\Gamma(t)$	External excitation torque	N·m
Ω	Constant angular velocity	rad/s

References

- [1] H. Frahm, Device for damping vibrations of bodies, in, Google Patents, 1911.
- [2] J. Ormondroyd, J. Den Hartog, The theory of the dynamic vibration absorber, *Journal of Fluids Engineering*, 49(2) (1928).
- [3] K. Iwanami, K. Seto, An optimum design method for the dual dynamic damper and its effectiveness, *Bulletin of JSME*, 27(231) (1984) 1965-1973.
- [4] T. Asami, Optimal design of double-mass dynamic vibration absorbers arranged in series or in parallel, *Journal of Vibration and Acoustics*, 139(1) (2017) 011015.
- [5] Y. Shen, H. Peng, X. Li, S. Yang, Analytically optimal parameters of dynamic vibration absorber with negative stiffness, *Mechanical Systems and Signal Processing*, 85 (2017) 193-203.
- [6] M.M. Nazari, A. Rahi, Parameters optimization of a nonlinear dynamic absorber for a nonlinear system, *Archive of Applied Mechanics*, 93(8) (2023) 3243-3258.
- [7] W.-B. Shangguan, X.-Y. Pan, Multi-mode and rubber-damped torsional vibration absorbers for engine crankshaft systems, *International Journal of Vehicle Design*, 47(1-4) (2008) 176-188.
- [8] X.-T. Vu, D.-C. Nguyen, D.-D. Khong, V.-C. Tong, Closed-form solutions to the optimization of dynamic vibration absorber attached to multi-degrees-of-freedom damped linear systems under torsional excitation using the fixed-point theory, *Proceedings of the Institution of Mechanical Engineers, Part K: Journal of Multi-body Dynamics*, 232(2) (2018) 237-252.
- [9] V. Manchi, C. Sujatha, Torsional vibration reduction of rotating shafts for multiple orders using centrifugal double pendulum vibration absorber, *Applied Acoustics*, 174 (2021) 107768.
- [10] Y. Cao, H. Yao, J. Dou, C. Wu, Torsional vibration suppression of rotor systems using a rubber-based nonlinear energy sink, *Meccanica*, 58(4) (2023) 565-585.
- [11] B. Xiang, W. Wong, Electromagnetic vibration absorber for torsional vibration in high speed rotational machine, *Mechanical Systems and Signal Processing*, 140 (2020) 106639.
- [12] D.-C. Nguyen, Determination of optimal parameters of the tuned mass damper to reduce the torsional vibration of the shaft by using the principle of minimum kinetic energy, *Proceedings of the Institution of Mechanical Engineers, Part K: Journal of Multi-body Dynamics*, 233(2) (2019) 327-335.
- [13] Y. Shen, Z. Xing, S. Yang, J. Sun, Parameters optimization for a novel dynamic vibration absorber, *Mechanical Systems and Signal Processing*, 133 (2019) 106282.
- [14] X. Wang, B. Yang, H. Yu, Optimal design and experimental study of a multidynamic vibration absorber for multifrequency excitation, *Journal of Vibration and*

- Acoustics, 139(3) (2017) 031011.
- [15] Y. Chang, J. Zhou, K. Wang, D. Xu, A quasi-zero-stiffness dynamic vibration absorber, *Journal of sound and vibration*, 494 (2021) 115859.
- [16] Y. Cheung, W. Wong, Design of a non-traditional dynamic vibration absorber, *The Journal of the Acoustical Society of America*, 126(2) (2009) 564-567.
- [17] D. Tchokogoué, M. Mu, B.F. Feeny, B.K. Geist, S.W. Shaw, The effects of gravity on the response of centrifugal pendulum vibration absorbers, *Journal of Vibration and Acoustics*, 143(6) (2021) 061011.
- [18] M. Rao, C. Sujatha, Design of centrifugal pendulum vibration absorber to reduce the axial vibration of rotating shafts for multiple orders, *SAE International Journal of Passenger Cars-Mechanical Systems*, 13(06-13-02-0007) (2020) 81-105.
- [19] K. Kecik, Assessment of energy harvesting and vibration mitigation of a pendulum dynamic absorber, *Mechanical Systems and Signal Processing*, 106 (2018) 198-209.
- [20] A. El-Sayed, H. Bauomy, Vibration suppression of subharmonic resonance response using a nonlinear vibration absorber, *Journal of Vibration and Acoustics*, 137(2) (2015) 024503.
- [21] S.W. Shaw, R. Bahadori, Tuning of centrifugal pendulum vibration absorbers operating in a fluid, *Nonlinear Dynamics*, 112(2) (2024) 741-755.
- [22] T. Abu Seer, N. Vahdati, O. Shiryayev, Adaptive torsional tuned vibration absorber for rotary equipment, *Vibration*, 2(1) (2019) 116-134.
- [23] R. Faal, B. Crawford, R. Sourki, A. Milani, Experimental, numerical and analytical investigation of the torsional vibration suppression of a shaft with multiple optimal undamped absorbers, *Journal of Vibration Engineering & Technologies*, 9 (2021) 1269-1288.
- [24] S. Goodarzi, A. Rahi, Optimization of dual dynamic vibration absorber to reduce rotor torsional vibrations, *Journal of Vibration and Sound*, 13(26) (2025) 3-1.
- [25] J. Taghipour, M. Dardel, M.H. Pashaei, Vibration mitigation of a nonlinear rotor system with linear and nonlinear vibration absorbers, *Mechanism and Machine Theory*, 128 (2018) 586-615.
- [26] Y. Cao, Z. Li, J. Dou, R. Jia, H. Yao, An inerter nonlinear energy sink for torsional vibration suppression of the rotor system, *Journal of Sound and Vibration*, 537 (2022) 11718.
- [27] B. Al-Bedoor, K. Moustafa, K. Al-Hussain, Dual dynamic absorber for the torsional vibrations of synchronous motor-driven compressors, *Journal of sound and vibration*, 220(4) (1999) 729-748.
- [28] J.H. Ginsberg, *Advanced engineering dynamics*, Cambridge University Press, 1998.
- [29] A.H. Nayfeh, D.T. Mook, *Nonlinear oscillations*, John Wiley & Sons, 2008.
- [30] A.H. Nayfeh, *Perturbation methods in nonlinear dynamics*, in: *Lecture Notes in Physics: Nonlinear Dynamics Aspects of Particle Accelerators*, Springer, 2007, pp. 238-314.
- [31] H. Abundis-Fong, J. Enríquez-Zárate, A. Cabrera-Amado, G. Silva-Navarro, Optimum design of a nonlinear vibration absorber coupled to a resonant oscillator: A case study, *Shock and Vibration*, 2018(1) (2018) 2107607.
- [32] R. Hamming, *Numerical methods for scientists and engineers*, Courier Corporation, 2012.
- [33] R.S. Esfandiari, *Numerical methods for engineers and scientists using MATLAB®*, Crc Press, 2017.

HOW TO CITE THIS ARTICLE

S. Goodarzi, A. Rahi, *Torsional Vibration Reduction of a Rotor by Using Nonlinear Dual Dynamic Vibration Absorber*, *AUT J. Mech Eng.*, 10(1) (2026) 75-88.

DOI: [10.22060/ajme.2025.23992.6169](https://doi.org/10.22060/ajme.2025.23992.6169)

